PHYSICAL REVIEW E VOLUME 47, NUMBER 2 FEBRUARY 1993

Partition functions of rare-earth halide plasmas

R. Holbrook
Department of Aerospace Engineering, University of Southern California, Los Angeles, California 90089-1191

L. A. Kaledin*
Department of Chemistry, Massachusetts Institute of Technology, Cambridge, Massachusetts 02139

J. A. Kunc†
Institute for Theoretical Atomic and Molecular Physics, Harvard University and Smithsonian Astrophysical Observatory, Cambridge, Massachusetts 02138

(Received 13 July 1992)

The partition functions are calculated for gases consisting of Ln and X atoms and LnX molecules and their singly charged ions (Ln≡Dy,Ho,Tm and X≡I,Br).

PACS number(s): 51.30.+i, 52.25.Kn, 52.80.Yr, 05.70.Ce

I. INTRODUCTION

In this work, the equilibrium partition functions of monatomic (Dy,Ho,Tm and Dy^+,Ho^+,Tm^+) and diatomic (DyI,HoI,TmI,DyBr,HoBr,TmBr and DyI^+,HoI^+,TmI^+,$DyBr^+$,$HoBr^+$,$TmBr^+$) gases are calculated. The negative rare-earth halide LnX^- ions are not considered because of the lack of reliable spectroscopic data for these ions. (In most cases, negative ions do not influence the kinetic properties of low-temperature plasmas with high electron densities [1,2]. However, some negative molecular ions containing metal atoms can be stable [3].)

Knowledge of the partition functions studied here is essential for understanding some light sources operating on mixtures of mercury (the "background" gas) and rare-earth halide molecules LnX (Ln≡Dy,Ho,Tm, X≡I,Br). These sources have high radiative output power, but controllability of their frequency spectrum is poor because of the lack of thermodynamic and kinetic models of these plasmas. Even though rare-earth halide plasmas are of major importance in high-pressure light sources, neither statistical nor thermodynamic evaluations of the plasma partition functions are available at present.

The light sources based on the rare-earth halides have a broad range of pressure (typically, below 1 atm) and a gas temperature well below 10 000 K. In most cases, the source gas is close to local thermal equilibrium [4]. Therefore, one can assume that in the source $T_e = T_+ = T$, where T_e, T_+, and T are the temperatures of electrons, ions, and neutral species, respectively. Also, at high electron densities, the Debye radius is very small and the plasma is electrically neutral in all the regions where the model of local thermal equilibrium at temperature T is valid. Thus, one can say that $n_e = n_+$, where n_e and n_+ are the electron and positive-ion particle densities, respectively.

II. ATOMIC, MOLECULAR, AND IONIC QUANTUM STATES

The energy levels of the atoms and atomic ions considered here were taken from Ref. [5]. The rotational, vibrational, and electronic states of the rare-earth halide molecules are unknown. The calculation of the molecular rotational and vibrational spectroscopic constants and of the electronic levels is very difficult because of the large number of low-lying electronic states. Practically, the only approach capable of dealing with this problem (with an accuracy acceptable in the applications of the present work) is the ligand field theory [6,7]. In general, the ligand field model gives reliable predictions of electronic structures of heavy molecules with predominantly ionic chemical bonding. Thus, it is well suited to study the electronic structures of LnX and LnX^+ molecules [8,9].

III. LIGAND FIELD APPROACH

In the ligand field model, the low-lying molecular electronic states of LnX and LnX^+ are interpreted as electronic states of the Ln^+ and Ln^{2+} metal ions, respectively, perturbed by the strong electrostatic field of the X^- ion. All (two-center) metal-ligand exchange and overlap interactions are neglected. The ligand field has three important effects on the Ln^+ and Ln^{2+} states: (1) the relative energies of the Ln^+ and Ln^{2+} electronic configurations are altered in the X^- field and the compact $4f$ orbitals are destabilized much more than the more diffuse $6s$ orbitals [6]; (2) the L,S,J terms of each Ln^+ (or Ln^{2+}) configuration are split into their M_J components in the X^- field; (3) the ligand field causes some intra- and interconfiguration mixing. With X^- approximated as a point charge located at a distance $R_e^{(i)}$ from Ln^+ (or Ln^{2+}), the effects on the states of the metal ion can be evaluated quantitatively by expanding the electrostatic interaction in the spherical harmonics at the metal

 ©1993 The American Physical Society

TABLE I. The calculated energies (in cm^{-1}) of the DyX configurations below the ionization limit; g is the total statistical weight of the configuration, ΔE is the energy range of the states included in the configuration, and δE is the density of the states per 1000 cm^{-1}.

Configuration	Dy^+ [a]	DyBr	DyI	g	ΔE	δE
$f^{10}s$	0	0	0	2002	55 000	34.6
f^9s^2	12 300	900	1800	2002	35 000	57
f^9ds	10 600	3400	4100	40 040	75 000	534
f^9d^2	19 000	16 000	16 400	90 090	60 000	1500
$f^{10}d$	14 800	19 000	18 700	10 010	70 000	143
f^9ps	36 000	23 100	24 100	24 024	70 000	343
$f^{10}p$	25 200	23 700	23 800	6006	60 000	100
f^9dp	38 000	29 300	30 100	120 120	80 000	1500

[a]Reference [27].

center. $R_e^{(i)}$ is the equilibrium internuclear distance of the molecule in the ith electronic state [$i=1$ for the ground electronic state; we omit the superscript (i) in cases when $i=1$].

The ligand field Hamiltonian for the molecule LnX or the molecular ions LnX^+ is expressed as [6]

$$H=\sum_i C_0^k(\theta_i,\varphi_i)B_0^k(r_i)+H_{\mathrm{FI}} , \quad (1)$$

where the sum is over all of the electrons on the metal-ion center, C_0^k is a modified spherical harmonic, and B_0^k is a radial one-electron operator. H_{FI} is the total Hamiltonian of the free metal ion including all single-center electrostatic and spin-orbit interactions. The molecular electronic structure is best analyzed by partitioning the ligand field term into two parts: the monopolar term $C_0^0B_0^0$, and the higher terms $C_0^kB_0^k$.

The low-lying ionic configurations of Ln^+ are [5] $4f^N6s$ (ground configuration), $4f^{N-1}6s^2$, and $4f^{N-1}5d6s$. Simple electrostatic calculations show that the $4f^{N-1}6s^2$ and $4f^{N-1}5d6s$ configurations are stabilized (see Tables I–VI) in the field of the X^- point charge by 10 000 cm^{-1} and by 5000 cm^{-1} relative to the $4f^N6s$ configuration. The B_0^0 ligand field term is greater than zero (thus, totally destabilizing) and serves to reorder these configurations from their free-ion positions. In LnX with Ln in the second half of the lanthanide series, the Ln^+ $f^{N-1}s^2$ and f^Ns levels are predicted (see Table VII) to occur at the lowest energy. This stabilization of the $f^{N-1}s^2$ configuration relative to the f^Ns configuration originates from the difference in the B_0^0 term for the final metal-centered electron. The value of the B_0^0 term is significantly larger (that is, destabilizing) for the compact $4f$ orbitals ($\langle r^2\rangle^{1/2}=0.3$ Å) than, for example, the $6s$ orbital, where $\langle r^2\rangle^{1/2}=3.4$ Å (see Ref. [6]).

The second half of the $Ln^+(f^Ns)$ configuration is best described by the J,j atomic coupling scheme because of the large spin-orbit interaction between the $4f$ "core" electrons. The large spin-orbit interaction splits the f^N configuration into the $L_fS_fJ_f$ terms separated by about 4000 cm^{-1}. The $6s$ electron interacts weakly with the $4f$ electrons, through the electrostatic exchange term in the atomic Hamiltonian, to split the $^{2S+1}L_{J_f}$ levels into $J_a=J_f+\frac{1}{2}$ and $J_a=J_f-\frac{1}{2}$ atomic states. The Slater-Condon parameter that describes this splitting is the two-electron exchange integral $G_3(4f,6s)$ (see Table VIII).

IV. MOLECULAR STRUCTURE

The second part of the ligand field Hamiltonian serves to remove the $2J_a+1$ (the subscript a denotes atomic

TABLE II. The calculated energies (in cm^{-1}) of the HoX configurations below the ionization limit; g is the total statistical weight of the configuration, ΔE is the energy range of the states included in the configuration, and δE is the density of the states per 1000 cm^{-1}.

Configuration	Ho^+ [a]	HoBr	HoI	g	ΔE	δE
$f^{10}s^2$	10 000	0	0	1001	55 000	18
$f^{11}s$	0	1400	500	728	55 000	13
$f^{10}ds$	11 500	5700	5500	20 020	70 000	286
$f^{11}d$	15 800	21 400	20 200	3640	70 000	52
$f^{10}d^2$	23 000	21 400	20 900	45 045	80 000	563
$f^{11}p$	25 500	25 400	24 600	2184	65 000	34
$f^{10}ps$	34 000	22 500	22 600	12 012	70 000	172
$f^{10}dp$	39 000	31 700	31 600	72 072	80 000	900

[a]Reference [27].

TABLE III. The calculated energies (in cm^{-1}) of the TmX configurations below the ionization limit; g is the total statistical weight of the configuration, ΔE is the energy range of the states included in the configuration, and δE is the density of the states per 1000 cm^{-1}.

Configuration	Tm^+ [a]	TmBr	TmI	g	ΔE	δE
$f^{13}s$	0	0	0	28	10 000	2.8
$f^{12}s^2$	12 457	1057	1957	91	33 000	2.6
$f^{12}ds$	16 568	9400	10 100	1820	55 000	39
$f^{13}d$	17 625	21 800	21 500	140	20 000	7
$f^{13}p$	25 980	24 500	24 600	84	15 000	5.6
$f^{12}ps$	38 225	25 300	26 300	1092	40 000	27
$f^{12}d^2$	30 509	27 500	27 900	4095	60 000	68
$f^{12}dp$	44 838	36 100	36 900	5460	60 000	91
f^{14}	34 000	45 400	44 500	1	0	

[a]Reference [27].

TABLE IV. The calculated energies (in cm^{-1}) of the DyX^+ configurations below the ionization limit; g is the total statistical weight of the configuration, ΔE is the energy range of the states included in the configuration, and δE is the density of the states per 1000 cm^{-1}.

Configuration	Dy^{2+} [a]	$DyBr^+$	DyI^+	g	ΔE	δE
f^{10}	0	0	0	1001	50 000	20
f^9d	17 500	10 300	11 000	20 020	60 000	334
f^9s	25 000	13 600	14 500	4004	50 000	80
f^9p	60 000	47 100	48 100	12 012	65 000	185
f^8d^2	71 000	50 000	58 000	135 135	80 000	1690
f^8ds	91 000	72 400	74 000	60 060	80 000	750
f^8s^2	112 000	89 200	91 000	3003	40 000	75

[a]Reference [27].

TABLE V. The calculated energies (in cm^1) of the HoX^+ configurations below the ionization limit; g is the total statistical weight of the configuration, ΔE is the energy range of the states included in the configuration, and δE is the density of the states per 1000 cm^{-1}.

Configuration	Ho^{2+} [a]	$HoBr^+$	HoI^+	g	ΔE	δE
f^{11}	0	0	0	364	50 000	7.3
$f^{10}p$	57 500	44 600	45 600	6006	60 000	100
f^9d^2	79 000	64 600	66 000	90 090	60 000	1500
f^9ds	96 000	77 400	79 000	40 040	75 000	534
f^9s^2	117 000	94 200	96 000	2002	35 000	57
$f^{10}d$	18 100	10 900	11 600	10 010	70 000	143
$f^{10}s$	21 800	10 400	11 300	2002	55 000	35

[a]Reference [27].

TABLE VI. The calculated energies (in cm^{-1}) of the TmX^+ configurations below the ionization limit; g is the total statistical weight of the configuration, ΔE is the energy range of the states included the configuration, and δE is the density of the states per 1000 cm^{-1}.

Configuration	Tm^{2+} [a]	$TmBr^+$	TmI^+	g	ΔE	δE
f^{13}	0	0	0	14	10 000	1.4
$f^{12}p$	62 000	49 900	50 100	546	35 000	16
$f^{11}d^2$	85 000	70 600	72 000	16 380	70 000	234
$f^{11}ds$	100 000	81 400	83 000	7280	70 000	104
$f^{11}s^2$	115 000	82 200	94 000	364	50 000	7.3
$f^{12}d$	22 900	15 700	16 400	910	50 000	18
$f^{12}s$	25 300	13 900	14 800	182	35 000	5.2

[a]Reference [27].

TABLE VII. Stabilization energies (in cm^{-1}) for the second-half lanthanide series LnX molecules and their singly charged ions; r is the Ln-X distance in LnX_3 (gas phase) and $\gamma = r[\text{Gd-}X]/r[\text{Gd-F}]$.

X	r[Gd-X] (Å)	γ	f-s	d-s	p-s	f-d
F	2.053[a]	1	14 760	5460	−2000	9300
Cl	2.488[a]	1.22	12 100	4500	−1700	7600
Br	2.641[a]	1.3	11 400	4200	−1500	7200
I	2.840[a]	1.4	10 500	3900	−1400	6500

[a]Reference [14].

quantum number) degeneracy of the atomic states. The energy of a given $M_{J_a} = \Omega$ level is determined by the orientation of the f and d electrons relative to the negatively charged ligand. The magnitude of the splitting of the levels is largely determined by the magnitude of the radial one-electron ligand field parameter B_0^2. The effects of the higher-order terms (B_0^4 and B_0^6) in the point-charge expansion are significantly smaller than those of the leading quadrupolar (B_0^2) term.

The ligand field parameters, and therefore the magnitude of the splittings of the free-ion levels, can be computed by evaluating the radial integrals, using the Hartree-Fock wave functions, for the $4f$ electron-density distribution (Tables VIII and IX). These values can be inserted directly into the effective molecular Hamiltonian for the $4f^N6s$, $4f^{N-1}6s^2$, and $4f^{N+1}$ configurations, along with the values of $G_3(4f,6s)$ and $\xi(4f)$ obtained from the corresponding atomic spectra [10]. The energy levels up to 2000 cm^{-1} calculated in this way, with no adjustable parameters, are shown in Tables X–XV. Eight important configurations lie below the ionization limit V_{ion} of each LnX and LnX^+ molecule. The molecules DyX, HoX, and TmX (X=Br,Br^+,I,I^+) have about 100 000, 60 000, and 10 000 Ω-components [Hund's case (c)], respectively. In order to simplify calculations of the molecular partition functions, we combined all Ω-states above 2000 cm^{-1} and below 8000 cm^{-1} and placed them at energy 5000 cm^{-1}, with statistical weight corresponding to the total statistical weight of these states. Similarly, all Ω states above 8000 cm^{-1} and below 22 000 cm^{-1} were placed at the energy 15 000 cm^{-1}, all states above 22 000 cm^{-1} and below the V_{ion}(LnX) and 48 000 cm^{-1} for LnX^+ were placed at energy 35 000 cm^{-1}, and all states LnX^+ above 48 000 cm^{-1} and below the V_{ion}(LnX^+) were placed at energy 75 000 cm^{-1}. [We took the ionization potential $V_{\text{ion}}(\text{Ln}X^+) \simeq V_{\text{ion}}(\text{LnF}^+)$.]

TABLE VIII. The parameters (in cm^{-1}) for the Hamiltonian [Eq. (1)] for the ground f^Ns superconfiguration.

	DyBr	HoBr	TmBr	DyI	HoI	TmI
B_2	1173	1147	1077	954	922	864
B_4	75	72	64	53	50	44
B_6	9	9	8	6	5	5
ζ_{so}	1900	2170	2300	1900	2170	2300
G_3	150	150	150	150	150	150

TABLE IX. The parameters (in cm^{-1}) for the Hamiltonian [Eq. (1)] for the ground f^Ns superconfiguration.

	$DyBr^+$	$HoBr^+$	$TmBr^+$	DyI^+	HoI^+	TmI^+
B_2	2550	2450	2180	2070	2070	1740
B_4	390	350	250	320	290	210
B_6	120	100	55	100	75	45
ζ_{s0}	1900	2170	2300	1900	2170	2300

In all these cases, the statistical weight of each combined state was taken as equal to the total statistical weight of all the combined states.

The vibrational frequencies and internuclear distances associated with the f^Ns, $f^{N-1}s^2$, and $f^{N-1}ds$ molecular configurations are not expected to be very different near the Ln^+X^- atomic-ion-in-molecule limit. Using the existing experimental data for the LnF and LnF^+ molecules (Table XVI), we estimated the spectroscopic constants of the LnX and LnX^+ molecules (Tables XVII and XVIII, respectively).

Dissociation energies of the LnX and LnX^+ molecules were calculated by using the following simplified model [11,12]. Since the LnX molecules with $X \equiv$I,Br have f^Ns-type ground configurations, we are interested in the

TABLE X. The calculated term energies $T_e^{(i)}$ (in cm^{-1}), the statistical weights g_i, $\Omega^{(i)}$-numbers, and configurational parentage labels y_i for the DyBr and DyI molecules.

DyBr				DyI			
$T_e^{(i)}$	g_i	$\Omega^{(i)}$	y_i	$T_e^{(i)}$	g_i	$\Omega^{(i)}$	y_i
0	2	8.5	1	0	2	8.5	1
65	2	7.5	1	52	2	7.5	1
116	2	6.5	1	93	2	6.5	1
157	2	5.5	1	126	2	5.5	1
189	2	4.5	1	152	2	4.5	1
215	2	3.5	1	173	2	3.5	1
234	2	2.5	1	189	2	2.5	1
247	2	1.5	1	200	2	1.5	1
253	2	0.5	1	205	2	0.5	1
622	2	7.5	1	621	2	7.5	1
693	2	6.5	1	677	2	6.5	1
747	2	5.5	1	721	2	5.5	1
788	2	4.5	1	754	2	4.5	1
820	2	3.5	1	781	2	3.5	1
844	2	2.5	1	800	2	2.5	1
860	2	1.5	1	817	2	1.5	1
868	2	0.5	1	820	2	0.5	1
900	2	7.5	2	1800	2	7.5	2
1062	2	6.5	2	1932	2	6.5	2
1200	2	5.5	2	5000	2100		
1312	2	4.5	2	15 000	16 600		
1400	2	3.5	2	35 000	80 000		
1465	2	2.5	2				
1506	2	1.5	2				
1527	2	0.5	2				
5000	2100						
15 000	16 600						
35 000	80 000						

TABLE XI. The calculated term energies $T_e^{(i)}$ (in cm^{-1}), the statistical weights g_i, $\Omega^{(i)}$-numbers, and configurational parentage labels y_i for the HoBr and HoI molecules.

HoBr				HoI			
$T_e^{(i)}$	g_i	$\Omega^{(i)}$	y_i	$T_e^{(i)}$	g_i	$\Omega^{(i)}$	y_i
0	2	8	2	0	2	8	2
68	2	7	2	53	2	7	2
120	2	6	2	95	2	6	2
161	2	5	2	128	2	5	2
193	2	4	2	154	2	4	2
217	2	3	2	174	2	3	2
235	2	2	2	188	2	2	2
245	2	1	2	196	2	1	2
249	1	0	2	199	1	0	1
1400	1	0	1	500	1	0	1
1404	2	1	1	503	2	1	2
1414	2	2	1	511	2	2	2
1431	2	3	1	525	2	3	2
1456	2	4	1	545	2	4	2
1487	2	5	1	571	2	5	2
1528	2	6	1	604	2	6	2
1580	2	7	1	646	2	7	2
1649	2	8	1	699	2	8	2
1869	1	0	1	969	1	0	1
1874	2	1	1	973	2	1	2
1887	2	2	1	983	2	2	2
1910	2	3	1	1002	2	3	2
1941	2	4	1	1027	2	4	2
1983	2	5	1	1061	2	5	2
5000	800			1106	2	6	2
15 000	5070			1164	2	7	2
35 000	43 000			5000	800		
				15 00	5070		
				35 000	43 000		

TABLE XII. The calculated term energies $T_e^{(i)}$ (in cm^{-1}), the statistical weights g_i, $\Omega^{(i)}$- numbers, and configurational parentage labels y_i for the TmBr and TmI molecules.

TmBr				TmI			
$T_e^{(i)}$	g_i	$\Omega^{(i)}$	y_i	$T_e^{(i)}$	g_i	$\Omega^{(i)}$	y_i
0	1	0	1	0	1	0	1
28	2	1	1	24	2	1	1
137	2	2	1	111	2	2	1
170	1	0	1	170	1	0	1
255	2	1	1	235	2	1	1
337	2	3	1	271	2	3	1
469	2	2	1	405	2	2	1
618	2	4	1	495	2	4	1
772	2	3	1	651	2	3	1
1057	1	0	2	1957	1	0	2
1071	2	1	2	1971	2	1	2
1115	2	2	2	5000	40		
1190	2	3	2	15 000	480		
1302	2	4	2	35 000	4300		
1452	2	5	2				
1644	2	6	2				
5000	40						
15 000	480						
35 000	4300						

TABLE XIII. The calculated term energies $T_e^{(i)}$ (in cm^{-1}), the statistical weights g_i, and the $\Omega^{(i)}$-numbers for the $DyBr^+$ and DyI^+ molecular ions.

$DyBr^+$			DyI^+		
$T_e^{(i)}$	g_i	$\Omega^{(i)}$	$T_e^{(i)}$	g_i	$\Omega^{(i)}$
0	2	8	0	2	8
75	2	7	59	2	7
132	2	6	105	2	6
176	2	5	141	2	5
210	2	4	169	2	4
237	2	3	191	2	3
256	2	2	206	2	2
268	2	1	216	2	1
272	1	0	219	1	0
5000	120		5000	120	
15 000	5000		15 000	5000	
35 000	12 000		35 000	12 000	
75 000	97 000		75 000	97 000	

TABLE XIV. The calculated term energies $T_e^{(i)}$ (in cm^{-1}), the statistical weights g_i, and the $\Omega^{(i)}$-numbers for the $HoBr^+$ and HoI^+ molecular ions.

$HoBr^+$			HoI^+		
$T_e^{(i)}$	g_i	$\Omega^{(i)}$	$T_e^{(i)}$	g_i	$\Omega^{(i)}$
0	2	0.5	0	2	0.5
9	2	1.5	7	2	1.5
26	2	2.5	21	2	2.5
51	2	3.5	41	2	3.5
85	2	4.5	69	2	4.5
129	2	5.5	104	2	5.5
187	2	6.5	151	2	6.5
266	2	7.5	212	2	7.5
5000	44		5000	44	
15 000	2100		15 000	2100	
35 000	5400		35 000	5400	
75 000	6500		75 000	6500	

TABLE XV. The calculated term energies $T_e^{(i)}$ (in cm^{-1}), the statistical weights g_i, and the $\Omega^{(i)}$-numbers for the $TmBr^+$ and TmI^+ molecular ions.

$TmBr^+$			TmI^+		
$T_e^{(i)}$	g_i	$\Omega^{(i)}$	$T_e^{(i)}$	g_i	$\Omega^{(i)}$
0	2	0.5	0	2	0.5
121	2	1.5	95	2	1.5
349	2	2.5	276	2	2.5
663	2	3.5	528	2	3.5
5000	6		5000	6	
15 000	170		15 000	170	
35 000	620		35 000	620	
75 000	8800		75 000	8800	

TABLE XVI. Molecular constants of LnF molecules (cm^{-1}).

LnF	$Ln^+(f^{N+1}s)F^-$		$Ln^+(f^Nds)F^-$		$Ln^+(f^Ns^2)F^-$	
	R_e (Å)	$\Delta G_{1/2}$	R_e (Å)	$\Delta G_{1/2}$	R_e (Å)	$\Delta G_{1/2}$
BaF	2.159 27[a]	465.3[a]				
LaF			2.055[a]	537.1[a]	2.025[a]	570[a]
CeF			2.046[b]	543.8[c]		
EuF	2.080[d]	493.1[d]				
GdF			2.000[d]	557.3[d]	1.965[d]	602.1[d]
TbF					1.960[e]	611.1[e]
DyF	2.007[c]	505.0[c]			1.905[c]	605.0[c]
HoF					1.940[c]	615.3[c]
YbF	2.016[a]	501.9[a]				
LuF					1.917[a]	611.8[a]

[a]Reference [13].
[b]Reference [28].
[c]Reference [31].
[d]Reference [29].
[e]Reference [30].

dissociation energies for the following processes:

$$Ln^+(f^Ns)X^- \rightarrow Ln(f^Ns^2)+X(p^5) \ . \tag{2}$$

However, the DyF, HoF, and TmF molecules have the $Ln^+(f^{N-1}s^2)F^-$-type ground configuration. Values of D_0^0 for the $Ln^+(f^Ns)F^-$ molecules with Ln≡Dy,Ho,Tm can be obtained, by interpolation, from a plot of $D_0^0[Ln^+(f^Ns)F^-]$ versus N (for Ln≡Ba, Pr, Nd, Sm, Eu, and Yb) because all these molecules have the f^Ns ground configuration. Subsequently, we can scale the values of D_0^0 as follows:

$$\frac{D_0^0(LnX)}{D_0^0(LnF)}=\frac{D_0^0(BaX)}{D_0^0(BaF)}=\lambda \ , \tag{3}$$

where values of $D_0^0(BaX)$ are taken from Ref. [13]. The calculated dissociation energies D_0^0 are shown in Tables XIX and XX.

Values of the $(f\text{-}s)$, $(d\text{-}s)$, $(p\text{-}s)$, and $(f\text{-}d)$ stabilization energies are roughly proportional to $[R_e^{(i)}]^{-1}$. Unfortunately, the values of R_e in the LnX molecules having X≡I,Br are not available. Therefore, we assume that these distances are equal to the average Ln-X distance resulting from electronographic studies of LnX_3 (where Ln≡Gd) [14]. Subsequently, one can scale the values of the stabilization energies as follows (E^S_{LnX} denotes the stabilization energy of the LnX molecule):

$$\frac{E^S_{LnX}(f\text{-}s)}{E^S_{LnF}(f\text{-}s)}\simeq\frac{R_e(LnF)}{R_e(LnX)}=\frac{1}{\gamma} \ , \tag{4}$$

$$\frac{E^S_{LnX}(d\text{-}s)}{E^S_{LnF}(d\text{-}s)}\simeq\frac{1}{\gamma} \ , \tag{5}$$

and so on.

The stabilization energy of the second half of LnF was calculated in Ref. [15] as $E^S_{LnF}(d\text{-}s)=5000\ cm^{-1}$, while the calculated (from the lowest states of configurations $f^{10}s$ and f^9s^2 of Dy^+ and DyF) value of $E^S_{LnF}(f\text{-}s)=14760\ cm^{-1}$ (the latter value was calculated in Ref. [16] as 12 400 cm^{-1}). Thus,

$$E^S_{LnF}(f\text{-}d)=E^S_{LnF}(f\text{-}s)-E^S_{LnF}(d\text{-}s)=9760\ cm^{-1} \ . \tag{6}$$

This value is close to the experimental value of the stabilization energy for the LaF^+ molecule, $E^S_{LnF^+}(f\text{-}d)=9300\ cm^{-1}$. Therefore, we assume in our calculations that $E^S_{LnF}(f\text{-}d)=E^S_{LnF^+}(f\text{-}d)$. Since $4f$ and $5d$ are inner

TABLE XVII. The spectroscopic constants of the rare-earth halide molecules in the ground electronic states; V_{ion} is the ionization potential, and the other constants have their usual meaning.

	DyBr	HoBr	TmBr	DyI	HoI	TmI
D_0^0 (cm^{-1})	25 700	25 400	24 400	21 400	21 100	20 300
V_{ion} (cm^{-1})	46 900	47 600	49 000	47 200	47 700	49 200
ω_e (cm^{-1})	219	219	219	157	157	157
$\omega_e x_e$ (cm^{-1})	0.4	0.4	0.4	0.4	0.4	0.4
R_e (Å)	2.66	2.64	2.62	2.85	2.84	2.82
μ (a.w.u.)	53.56	53.83	54.24	71.26	71.72	72.47
$B_e(10^{-2}\ cm^{-1})$	4.45	4.49	4.53	2.9	2.9	2.9
$\alpha_e(10^{-4}\ cm^{-1})$	1.1	1.1	1.1	0.6	0.6	0.6

TABLE XVIII. The spectroscopic constants of the rare-earth halide molecular ions in the ground electronic states; V_{ion} is the ionization potential, and the other constants have their usual meaning.

	$DyBr^+$	$HoBr^+$	$TmBr^+$	DyI^+	HoI^+	TmI^+
D_0^0 (cm^{-1})	26 500	26 200	25 200	22 000	21 700	20 900
V_{ion} (cm^{-1})	94 100	95 200	97 200	94 100	95 200	97 200
ω_e (cm^{-1})	246	246	246	176	176	176
$\omega_e x_e$ (cm^{-1})	0.6	0.6	0.6	0.35	0.35	0.35
R_e (Å)	2.58	2.56	2.54	2.77	2.76	2.74
μ (a.w.u.)	53.56	53.83	54.24	71.26	71.72	72.47
B_e (10^{-2} cm^{-1})	4.72	4.76	4.80	3.07	3.07	3.07
α_e (10^{-4} cm^{-1})	1.4	1.4	1.4	0.76	0.76	0.76

orbitals, this assumption seems to be reasonable. Consequently, one has $E^S_{LnF}(d\text{-}s)=E^S_{LnF}(f\text{-}s)-E^S_{LnF}(f\text{-}d)$. The obtained values of the stabilization energies for the $(f\text{-}s)$, $(d\text{-}s)$, $(p\text{-}s)$, and $(f\text{-}d)$ configurations of the LnX molecules and singly charged molecular ions are given in Table VII.

As said before, the lowest electronic configuration for DyI, HoI, TmI, DyBr, HoBr, and TmBr molecules is $4f^N6s$. Using this configuration, the ligand field parameters for the ground f^Ns configuration were calculated (see Table VIII), as well as the molecular electronic energies and the statistical weights of all states with energies up to 2000 cm^{-1}. We assumed, when calculating the spectroscopic constants, that the equilibrium internuclear distance in the LnX molecules is close to the Ln-X distance in the LnF_3 molecules in gaseous phase [14]. In our calculations, the following scaling law for the vibrational constants ω_e was utilized:

$$\frac{\omega_e(\mathrm{Ln}X)}{\omega_e(\mathrm{LnF})}\simeq\frac{\omega_e(\mathrm{Ba}X)}{\omega_e(\mathrm{BaF})}\ , \tag{7}$$

$$\frac{\omega_e(\mathrm{Ln}X^+)}{\omega_e(\mathrm{Ln}X)}\simeq\frac{\omega_e(\mathrm{LaF}^+)}{\omega_e(\mathrm{LaF})}\ , \tag{8}$$

and

$$\frac{R_e(\mathrm{Ln}X^+)}{R_e(\mathrm{Ln}X)}\simeq\frac{R_e(\mathrm{LaF}^+)}{R_e(\mathrm{LaF})}\ , \tag{9}$$

where Ln≡Dy,Ho,Tm and X≡I,Br; ω_e(LaF) and R_e(LaF) are given in Ref. [13], $\omega_e(\mathrm{LaF}^+)$ and $R_e(\mathrm{LaF}^+)$ in Ref. [17], and ω_e(LnX) and R_e(LnX) are given in Table XVII.

Calculation of the spectroscopic constants of the LnX molecules in the excited electronic states is difficult. However, taking the constants for the excited electronic states as equal to those for the molecular ground states introduces an inaccuracy in the partition functions that is acceptable in the applications [18]. Therefore, we assume in our calculations that the R dependences of the intramolecular potentials $U^{(i,j)}(R)$ (see below) for the electronic states of a LnX molecule are close to each other. The assumption that the spectroscopic constants of the upper electronic molecular states can be approximated by the corresponding constants for the molecular electronic ground state can be analyzed by using the integer-valence model [6]. The regularities in the vibrational frequencies (see Table XVI) of the LnF molecules suggest that the typical states of the lanthanide component (Ln^+) of the halide diatomic molecules in the gas phase do not differ much from the Ln^{3+} component existing in the condensed phase. In the diatomic molecules, the $6s$ orbitals are polarized into the region behind the Ln ion, exposing the Ln ion (the charge on the X ligand is equal to $1e$) to an effective charge larger by $+1$ or $+2$ than it would be in the "formal" ionic model of Ln^+X^- (see Fig. 1). The $Ln^+(f^Ns)$ component "looks" to the X^- component like a doubly ionized ion, while the $Ln^+(f^{N-1}s^2)$ component "looks" like a triply ionized ion.

The vibrational spectroscopic constants can be given as

$$\omega_e\sim f_e^{1/2}\sim\left[\frac{Z_{\mathrm{Ln}}Z_X e^2}{R_e^2}\right]^{1/2}\ , \tag{10}$$

where f_e is the molecular force constant, and Z_{Ln} and Z_X are the charge numbers of Ln and X, respectively. In the integer valence model, the differences between the equilibrium internuclear distances for electronic configurations are within 5%, so one can assume that

$$\frac{R_e(f^Ns)}{R_e(f^{N-1}s^2)}\approx 1\ . \tag{11}$$

TABLE XIX. Dissociation energies D_0^0[LnX] (in cm^{-1}); $\lambda=D_0^0[\mathrm{Ba}X]/D_0^0[\mathrm{BaF}]$.

X	Ba	λ	Dy	Ho	Tm
F	47 600[a]	1	41 800[b]	41 200[b]	39 600[b]
Cl	35 700[a]	0.75	31 400	30 900	29 700
Br	29 300[a]	0.616	25 700	25 400	24 400
I	24 400[a]	0.513	21 400	21 100	20 300

[a]Reference [13].
[b]Corresponds to the process $Ln^+(f^Ns)F^-\rightarrow Ln(f^Ns^2)+F(p^5)$.

TABLE XX. Dissociation energies D_0^0[LnX^+] (in cm^{-1}). $D_0^0[\mathrm{Ln}X^+]=D_0^0[\mathrm{Ln}X]+V_{ion}[\mathrm{Ln}]-V_{ion}[\mathrm{Ln}X]$; V_{ion} is the ionization potential.

X^+	Dy	Ho	Tm
Br^+	26 500	26 200	25 200
I^+	22 000	21 700	20 900

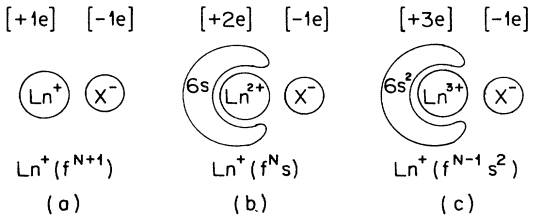

FIG. 1. Polarization of the 6*s* orbitals of the Ln^+ ion in the Ln*X* molecules: (a) no 6*s* orbitals, (b) one 6*s* orbital, (c) two 6*s* orbitals.

Thus, the ratio of ω_e for the $f^{N-1}s^2$ configuration to ω_e for the $f^N s$ configuration is close to

$$\frac{\omega_e(f^{N-1}s^2)}{\omega_e(f^N s)}=(\tfrac{3}{2})^{1/2}\frac{R_e(f^N s)}{R_e(f^{N-1}s^2)}\simeq 1.22 \ . \tag{12}$$

At high temperatures, one can assume [19] that

$$Q_{\text{vib}}=kT/hc\omega_e \ , \quad Q_{\text{rot}}=kT/hcB_e \ , \tag{13}$$

where Q_{vib} and Q_{rot} are vibrational and rotational molecular partition functions, respectively, k is the Boltzmann constant, h is Planck's constant, and c is the speed of light. Using the above, one can estimate the high-temperature (say, $T=7000$ K) ratio of the vibrational partition functions for the $Ln^+(f^{N-1}s^2)X^-$ and $Ln^+(f^N s)X^-$ configurations as

$$\frac{Q_{\text{vib}}[Ln^+(f^{N-1}s^2)X^-]}{Q_{\text{vib}}[Ln^+(f^N s)X^-]}\simeq(1.22)^{-1} \ . \tag{14}$$

Thus, one introduces less than about 22% inaccuracy in the vibrational partition functions when assuming that the vibrational spectroscopic constants $\omega_e^{(i)}$ of the upper electronic states of the molecules considered here are the same as the vibrational constants of the electronic ground states of the molecules.

As indicated above, the equilibrium internuclear distances $R_e^{(i)}$ for different electronic configurations differ by about 5%, and the rotational spectroscopic constants B_e differ by about 10%. Consequently, the ratio of the rotational partition functions for the $Ln^+(f^{N-1}s^2)X^-$ and $Ln^+(f^N s)X^-$ configurations is

$$\frac{Q_{\text{rot}}[Ln^+(f^{N-1}s^2)X^-]}{Q_{\text{rot}}[Ln^+(f^N s)X^-]}=\frac{B_e(f^N s)}{B_e(f^{N-1}s^2)}$$

$$=\frac{R_e^2(f^{N-1}s^2)}{R_e^2(f^N s)}\simeq 0.9 \ , \tag{15}$$

because

$$B_e\sim\frac{1}{R_e^2} \ . \tag{16}$$

Thus, one introduces less than about a 10% inaccuracy in the rotational partition functions when assuming that the rotational spectroscopic constants B_e of the upper electronic states of the molecules considered here are the same as the rotational constants of the electronic ground states of the molecules.

V. PRESSURE IONIZATION AND PRESSURE DISSOCIATION

The potential distribution in and around a particle immersed in plasma is influenced by its own bound electrons, free electrons, and free ions, and by bound electrons of other heavy particles. Any particle exposed to these interactions requires less energy to be ionized (the pressure ionization) than the energy needed for ionization when the particle is in a vacuum. Similar remarks can be made about the influence of the plasma interactions on the dissociation energies (the pressure dissociation) of molecules and molecular ions.

The pressure ionization and pressure dissociation in dense gases and plasmas are a very complex problem. All existing theories do not include external field and boundary effects, and they assume that the gas contains only "free" particles (free electrons, ions, and neutral ions) and "bound" particles (the electrons and nuclei in the heavy particles). Consequently, the interactions between particles are divided into three categories: (1) "free-free" interactions neglecting strong correlations and quantum-mechanical effects, (2) "free-bound" interactions (which are also responsible for the broadening and shift of the energy levels), and (3) "bound-bound" interactions. Even though such a classification includes most of the plasma particles, it is incomplete and ambiguous, because there can be a group of particles that are neither completely free nor completely bound, and that can be treated in terms of weak or strong pair correlations. (However, a satisfactory quantum-mechanical theory for the kinetics of particles with higher-order correlations is not available.) In addition, the electrons can be "free" for one phenomenon (for example, pressure) but not necessarily so for another (for example, conductivity). Adding to the difficulty in the description of the electric potentials in the vicinity of interacting particles, it is obvious that the concepts of the pressure ionization and the pressure dissociation have some uncertainty in their definitions and their numerical values.

If we denote the series limit $i\rightarrow\infty$ (equal to the ionization energy of the particle under consideration) by $E_0=V_{\text{ion}}$, then the highest energy level existing in the particle (as a result of the reduction of the ionization energy) will have the energy ε_n (with respect to the particle ground state) equal to

$$\varepsilon_n=E_0-\Delta\varepsilon_n \ , \tag{17}$$

where $\Delta\varepsilon_n$ represents the reduction of the ionization energy, and i and n denote energy levels ($i=1$, for the ground state).

Different models of the reduction of the ionization energy are discussed in Ref. [20]. We chose for our calculations the model of Ecker and Kroll [21] because this model seems to be the most consistent. Using a combination of statistical and thermodynamic approaches, Ecker

and Kroll developed a method to estimate the reduction of the ionization energy by the microfields of plasma charges. They employed the semiclassical approximation and formulated a generalized Saha equation as a function of the Helmholtz free energy and, consequently, as a function of the chemical potentials of the plasma components. The electrostatic contribution to the plasma chemical potentials was then expressed in terms of the average electrostatic micropotentials (obtained from a solution of the Poisson equation) at a given plasma particle. The final expression of the Ecker and Kroll model for the reduction of the ionization energy of a particle in plasma in local thermal equilibrium is given as

$$\Delta\varepsilon_n = \begin{cases} e^2/\rho_D & \text{when } N_e \le N_{\rm cr} , \\ G_k e^2/d_e & \text{when } N_e > N_{\rm cr} , \end{cases} \tag{18}$$

where N is the electron density,

$$d_e = \left[\frac{3}{4\pi N_e}\right]^{1/3} , \tag{19}$$

$$G_k = 2.2\frac{(2N_{\rm cr}e^2)^{1/2}}{N_{\rm cr}^{1/3}(kT)^{1/2}} , \tag{20}$$

and the critical density $N_{\rm cr}$ is

$$N_{\rm cr} = \frac{3}{4\pi}\left[\frac{kT}{e^2}\right]^3 . \tag{21}$$

The dependence of the reduction energy $\Delta\varepsilon_n$ on plasma temperature T and density N_e is given in Fig. 2. As can be seen from there, the pressure ionization has little impact on the partition functions as long as the electron density in the gas is not too high.

As discussed above, any molecule exposed to plasma interactions requires less energy to be dissociated than is needed for dissociation of the molecule in a vacuum. However, the reduction of the dissociation energy in the plasmas considered is negligible [22].

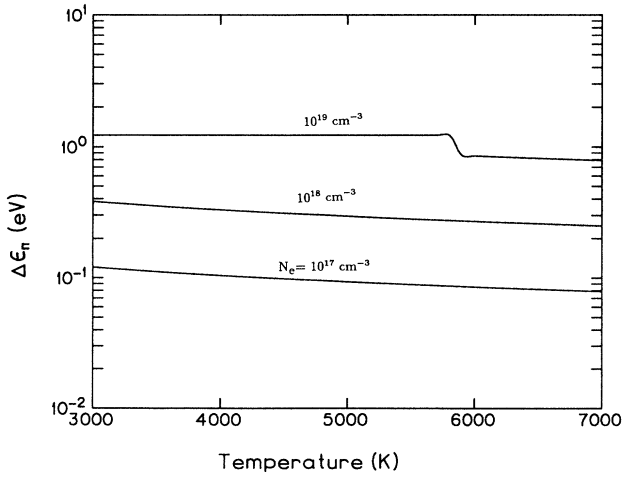

FIG. 2. Typical reduction, resulting from the presence of charged particles in the plasma, of the ionization energy of the LnX molecules; N_e is the electron density.

VI. PARTITION FUNCTIONS

The total energy ε_a of an atom is

$$\varepsilon_a = \varepsilon_{\rm tr} + \varepsilon_{\rm el} + \varepsilon_s , \tag{22}$$

where $\varepsilon_{\rm tr}$ and $\varepsilon_{\rm el}$ are translational and electronic energies, respectively, and ε_s is the nuclear-spin energy. Thus, the total atomic partition function Z can be taken as the product of the atomic translational partition function $Z_{\rm tr}$, the atomic electronic partition function $Z_{\rm el}$, and the nuclear-spin partition function Z_s,

$$Z = Z_{\rm tr}Z_{\rm el}Z_s , \tag{23}$$

where

$$Z_{\rm tr} = \frac{(2\pi mkT)^{3/2}V}{h^3} , \tag{24}$$

and

$$Z_{\rm el} = \sum_{i=1}^{i_m} g_i \exp(-\varepsilon_i/kT) , \tag{25}$$

where m is the mass of the atom, V is the volume occupied by the gas, g_i is the statistical weight of atomic level i of energy ε_i ($g_i = 2J_a + 1$, where J_a is the quantum number of the total electronic angular momentum of the atom in the ith level), and where the sum is taken over all (i_m) electronic levels existing in the atom. One should mention that if some levels, other than those given in Ref. [5] were added in the sum (25), then the partition function $Z_{\rm el}$ would be somewhat greater than that obtained in the present work.

The atomic (ionic) nuclear-spin partition function $Z_s^{(l)}$ for the lth atomic (ionic) isotope is

$$Z_s^{(l)} = 2I_s^{(l)} + 1 , \tag{26}$$

where $I_s^{(l)}$ is the spin quantum number of the atomic nucleus of the isotope. (The natural abundance of the Ln and X isotopes is given in Table XXI.)

TABLE XXI. Atomic constants. Z is the atomic number, A_l is the mass number of the lth isotope, M_l is the isotope atomic mass, $I_s^{(l)}$ is the corresponding nuclear spin, and a_l is the natural abundance (fraction) of the lth isotope.

Atom	Z	A_l	M_l	a_l	$I_s^{(l)}$
Dy	66	160	159.925 193	0.023	0
	66	161	160.926 930	0.189	$\frac{5}{2}$
	66	162	161.926 795	0.255	0
	66	163	162.928 728	0.249	$\frac{5}{2}$
	66	164	163.929 171	0.282	0
Ho	67	165	164.930 319	1.000	$\frac{7}{2}$
Tm	69	169	168.934 212	1.000	$\frac{1}{2}$
Br	35	79	78.918 336	0.507	$\frac{3}{2}$
	35	81	80.916 289	0.493	$\frac{3}{2}$
I	53	127	126.904 473	1.000	$\frac{5}{2}$

The expressions for translational, electronic, and nuclear-spin partition functions of atomic ions are similar to those given by Eqs. (24), (25), and (26), respectively; the ionic partition functions will be denoted hereafter by the superscript + (Z_{tr}^{+}, Z_{el}^{+}, and $Z_s^{+}=Z_s$).

Plots of the electronic partition functions Z_{el} for the rare-earth halide atoms and ions can be found in Fig. 3. The temperature range for these functions (and for the other partition functions of this work) is from 3000 to 7000 K.

The total energy of a diatomic molecule is assumed to be

$$\varepsilon_m=\varepsilon_{tr}+\varepsilon_{el}+\varepsilon_{vib,rot}+\varepsilon_s\ , \tag{27}$$

where ε_{tr} and ε_{el} are translational and electronic energies, respectively, $\varepsilon_{vib,rot}$ is the vibrational-rotational energy of the molecule in the given electronic state, and ε_s is the nuclear-spin energy. Therefore, the total molecular partition function Q_{tot} can be written as

$$Q_{tot}=Q_{tr}Q_{el}Q_{vib,rot}Q_s\ , \tag{28}$$

where Q_{tr}, Q_{el}, $Q_{vib,rot}$, and Q_s are the molecular translational, electronic, vibrational-rotational, and nuclear-spin partition functions, respectively.

The molecular translational partition functions Q_{tr} can be obtained from an expression similar to that given in Eq. (24), with m being the mass of the molecule under consideration.

The lowest level of the internal (electronic + vibrational + rotational) energy of a diatomic molecule is denoted by $i=1$ (the electronic ground state), $v=0$ (the vibrational ground state), and $J=\Omega^{(1)}$ (the rotational ground state), where v is the vibrational quantum number and J is the molecular rotational quantum number ($J=\Omega, \Omega+1, \Omega+2, \ldots$). The level ($i=1$, $v=0$, and $J=\Omega^{(1)}$) of the molecular energy is denoted in Fig. 4 as the level O^{II}; it is convenient to use the bottom of the $i=1, J=\Omega^{(1)}$ intramolecular potential curve

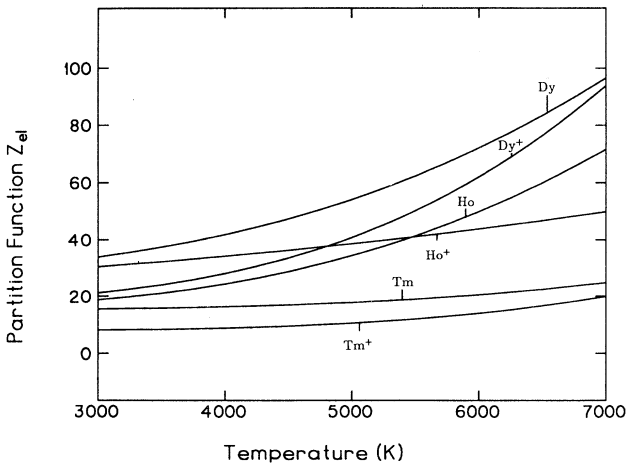

FIG. 3. Electronic partition functions for Ln and Ln^{+} atoms and ions.

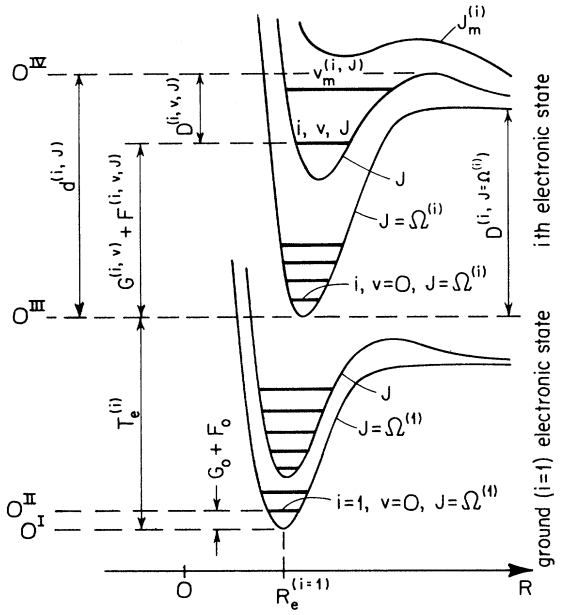

FIG. 4. Some intramolecular potentials $U^{(i,J)}(R)$ for the ground ($i=1$) and for an excited (i) electronic state of a diatomic molecule. R is the internuclear distance.

$U^{(i=1,J=\Omega^{(1)})}(R)$ as the reference level (the level O^{I} in Fig. 4) in consideration of the molecular energy.

The lowest curve, representing the intramolecular potential in the molecules in the ith electronic state, is the curve with $J=\Omega^{(i)}$ (see Fig. 4). As the rotational energy of the molecule increases, the well depth of the potential becomes shallower, which reflects the increasing (with J) contribution of the centrifugal energy. This contribution causes the dissociation energy $D^{(i,v,J)}$ of the molecule in a given i,v,Jth electronic-vibrational-rotational state to be a reciprocal function of the rotational quantum number J. (The dissociation energies of the rare-earth halide molecules and their ions in the ground electronic-vibrational-rotational states are given in Tables XVII and XVIII, respectively.) One can see from Fig. 4 that a molecule in the ith electronic state and in the (v,J)th vibrational-rotational state is stable if its vibrational-rotational energy level $G^{(i,v)}+F^{(i,v,J)}$ is below the corresponding dissociation limit (the level O^{IV} in Fig. 4). If $G^{(i,v)}+F^{(i,v,J)}$ becomes greater than $d^{(i,J)}$, the molecule dissociates.

A particular (i,v,J)th energy level (the thick horizontal line denoted by i,v,J in Fig. 4) of a molecule can be given as

$$\varepsilon^{(i,v,J)}=T_e^{(i)}+G^{(i,v)}+F^{(i,v,J)}-G_0-F_0\ , \tag{29}$$

where

$$G_0=G^{(i=1,\,v=0)},\quad F_0=F^{(i=1,\,v=0,\,J=\Omega^{(1)})}\ , \tag{30}$$

where all quantities are in cm^{-1}; $T_e^{(i)}$ is the energy difference (see Fig. 4) between the minima of the intramolecular potential curves of the $(i,J=\Omega^{(i)})$ and the $(i=1,\ J=\Omega^{(1)})$ molecular states; $G^{(i,v)}$ is the vibrational

energy, measured from the bottom of the intramolecular potential curve, of the molecule in the ith electronic and vth vibrational state; $F^{(i,v,J)}$ is the rotational energy of the molecule in the ith electronic, vth vibrational, and Jth rotational state.

The vibrational and rotational energy levels can be given, respectively, as

$$G^{(i,v)}=\omega_e^{(i)}(v+\tfrac{1}{2})-\omega_e x_e^{(i)}(v+\tfrac{1}{2})^2+\cdots , \tag{31}$$

$$F^{(i,v,J)}=B^{(i,v)}[J(J+1)-(\Omega^{(i)})^2]-D_e^{(i)}J^2(J+1)^2+\cdots , \tag{32}$$

where

$$B^{(i,v)}=B_e^{(i)}-\alpha_e^{(i)}(v+\tfrac{1}{2}) . \tag{33}$$

Taking the above into account, the internal (electronic-vibrational-rotational) partition function of a diatomic molecule can be given, neglecting the nuclear-spin partition function, as

$$Q_{\text{int}}=\sum_{i=1}^{i_m}\sum_{J=\Omega^{(i)}}^{J_m^{(i)}}\sum_{v=0}^{v_m^{(i,J)}}p(i,v,J)\times\exp\{-hc[T_e^{(i)}+G^{(i,v)}+F^{(i,v,J)}-G_0-F_0]/kT\} , \tag{34}$$

where $p(i,v,J)$ is the statistical weight of the molecule excited to the (i,v,J)th electronic-vibrational-rotational level,

$$p(i,v,J)=g_i(2J+1) , \tag{35}$$

where

$$g_i=\begin{cases}1 & \text{if } \Omega^{(i)}=0\\ 2 & \text{otherwise} .\end{cases} \tag{36}$$

It should be mentioned that, because of the large number of rotational levels that can exist in the ith electronic state, the sum (34) is quite insensitive, in the temperature range considered here, to the correction term containing $(\Omega^{(i)})^2$; for almost all rotational levels, except the few lowest levels, one has $J(J+1)\gg(\Omega^{(i)})^2$.

The number i_m of electronic levels taken into consideration in the sum (34) is limited to the number of levels existing in the particular particle. As discussed earlier, this number may depend on the reduction of the particle ionization energy.

The maximum rotational quantum number $(J_m^{(i)})$ of the molecule in the ith electronic state can be calculated from the intramolecular potential curves for the state. The quantum number $J_m^{(i)}$ for a given electronic state is limited by the value of the molecular dissociation energy for the ith state; this dissociation energy depends on the centrifugal energy (see below) of the molecular rotation; that is, it depends on the rotational quantum number of the molecule (see Fig. 4).

The effective intramolecular potential $U^{(i,J)}$ of a molecule in the ith electronic level can be given as a sum of two parts,

$$U^{(i,J)}(R)=U_v^{(i)}(R)+U_r^{(i,J)}(R) , \tag{37}$$

where $U_v^{(i)}$ is the intramolecular potential curve for the molecule in the ground $(J=\Omega^{(i)})$ rotational level.

Assuming that the Morse rotating oscillator is an accurate model of the rotational-vibrational motion of the diatomic molecules considered here, the three-parameter Morse potential can be assumed for the term $U_v^{(i)}(R)$ in Eq. (37),

$$U_v^{(i)}(R)=D^{(i,J=\Omega^{(i)})}(1-e^{-\beta^{(i)}(R-R_e^{(i)})})^2 , \tag{38}$$

where $D^{(i,J=\Omega^{(i)})}$ is the dissociation energy, referred to the potential minimum, of the oscillator with $J=\Omega^{(i)}$, $R_e^{(i)}$ is the equilibrium bond length of the oscillator, and $\beta^{(i)}$ is the Morse constant.

Neglecting the higher-order terms, the second (centrifugal) part of the intramolecular potential (37) can be given as

$$U_r^{(i,J)}(R)=\frac{\hbar^2[J(J+1)-(\Omega^{(i)})^2]}{2\mu R^2} , \tag{39}$$

where

$$\mu=\frac{m_1m_2}{m_1+m_2} \tag{40}$$

is the reduced mass of the molecule.

Equations (31) and (32) are almost identical with the expressions for the vibrational-rotational eigenvalues obtained from a solution of the Schrödinger equation when the effective potential (37) is used. Since Eqs. (31) and (32) have been verified for a large number of diatomic molecules, one can use the potential (37) for the determination of the potential curves for the rotational-vibrational motion of the molecules.

The maximum vibrational quantum number $v_m^{(i,J)}$ of the molecule in the ith electronic level and the Jth rotational level can be obtained from the intramolecular potential $U^{(i,J)}(R)$ for the level [see Eq. (37)].

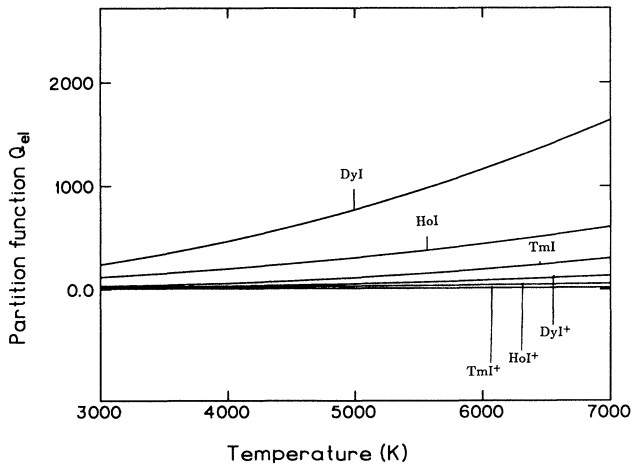

FIG. 5. Electronic partition functions for LnI and LnI^+ molecules and molecular ions.

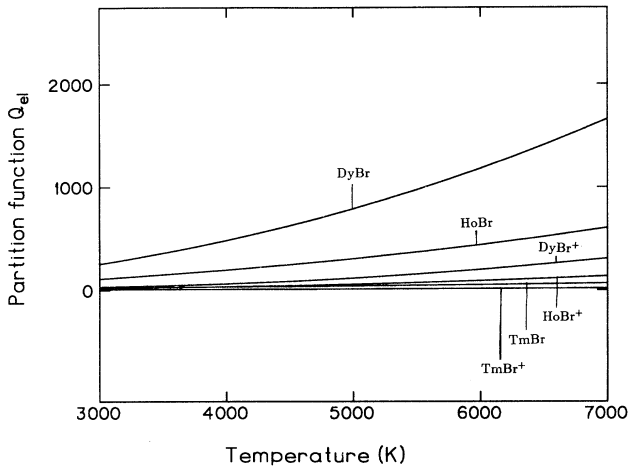

FIG. 6. Electronic partition functions for LnBr and $LnBr^+$ molecules and molecular ions.

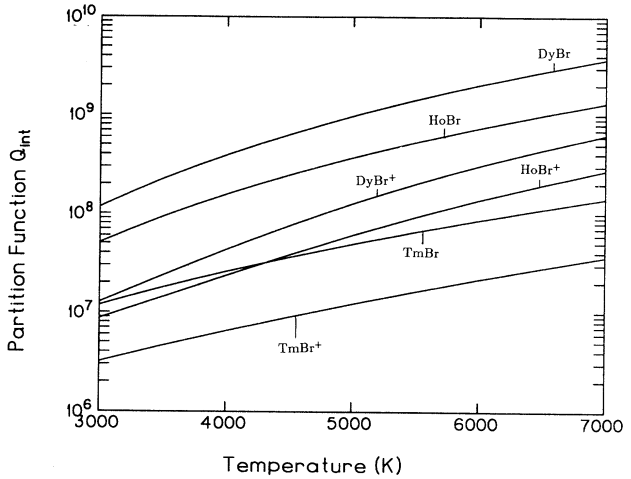

FIG. 8. Internal partition functions for LnBr and $LnBr^+$ molecules and molecular ions.

The components of the internal molecular partition function can be written as the following.

(1) The vibrational-rotational partition function of the molecules in the ith electronic state:

$$Q_{\text{vib,rot}}^{(i)} = \sum_{J=\Omega^{(i)}}^{J_m^{(i)}} \sum_{v=0}^{v_m^{(i,J)}} (2J+1)\exp\left[-\frac{hc}{kT}(G^{(i,v)}+F^{(i,v,J)} - G_0 - F_0)\right] . \tag{41}$$

(2) The electronic partition function of the molecules:

$$Q_{\text{el}} = \sum_{i=1}^{i_m} g_i \exp(-hcT_e^{(i)}/kT) . \tag{42}$$

The electronic partition functions Q_{el} for the rare-earth halide molecules and molecular ions considered in this work are given in Figs. 5 and 6.

(3) The internal partition functions $Q_{\text{int}} = Q_{\text{el}} Q_{\text{vib,rot}}$ for the rare-earth halide molecules and molecular ions are given in Figs. 7 and 8.

The nuclear-spin partition function Q_s of the (l,k)th isotope of a diatomic molecule is

$$Q_s^{(l,k)} = (2I_s^{(l)}+1)(2I_s^{(k)}+1) , \tag{43}$$

where $I_s^{(l)}$ and $I_s^{(k)}$ are spin quantum numbers of the molecular nuclei. (The natural abundance of the Ln and X isotopes is given in Table XXI.)

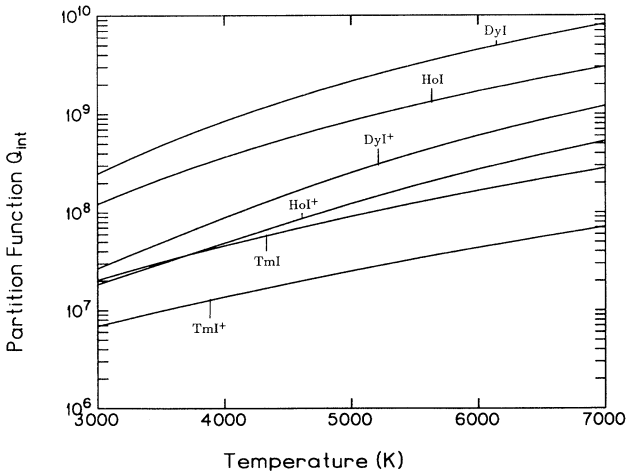

FIG. 7. Internal partition functions for LnI and LnI^+ molecules and molecular ions.

VII. ACCURACY AND VALIDITY OF THE PARTITION FUNCTIONS

The inaccuracy of the total partition functions of the rare-earth halides discussed in this work can be estimated by considering, for example, the corresponding inaccuracy for the DyI molecules at high temperature, say, $T=7000$ K (see Figs. 5–8). The internal molecular partition function (without the partition function associated with the nuclear spin) of DyI is

$$Q_{\text{int}} = Q_{\text{el}} Q_{\text{vib,rot}} \simeq 8.2\times 10^9 . \tag{44}$$

According to the previously discussed conclusions, the inaccuracies δQ_{rot} and δQ_{vib} of the rotational and vibrational partition functions at higher temperatures ($T\approx 7000$ K, the upper limit of the temperature considered in this work) are equal to 10% [Eq. (15)] and 22% [Eq. (12)], respectively. Let us assume that at $T\approx 7000$ K the relative accuracy of the electronic partition function Q_{el} is within a factor of 2. [One should add that the inaccuracy δQ_{el} (the major part of the inaccuracy δQ_{int}) is of much less importance in equilibrium calculations because, as a rule, the inaccuracy δZ_{el} of the atomic electronic partition function is close to δQ_{el} and they cancel each other.] Thus, the inaccuracy in calculating the molecular internal partition function should be less than

$\delta Q_{\text{int}} = 2 \times 1.1 \times 1.22 \simeq 2.7$ [$\ln(2.7) \simeq 1$] or $\delta Q_{\text{int}} = 0.5 \times 0.9 \times 0.78 \simeq 0.35$ [$\ln(0.35) \simeq -1$]. One of the most important and most frequently evaluated thermodynamic functions of gases in equilibrium is the gas free energy, which can be given as $F = -RT \ln(\delta Q_{\text{tot}})$, where R is the gas constant. The inaccuracy of calculating the function Q_{tot} is associated with the inaccuracy of calculating Q_{int}. Thus, $\delta F = \delta F_{\text{int}}$. Since $|F| > |F_{\text{int}}|$, the relative error of calculating the free energy F in the gases considered here is close to the ratio

$$\frac{|\delta F|}{|F|} < \frac{|\delta F_{\text{int}}|}{|F_{\text{int}}|} = \frac{\ln(\delta Q_{\text{int}})}{\ln(Q_{\text{int}})} \simeq \frac{1}{22.8} = 0.04 \ . \tag{45}$$

One should add that the rare-earth atoms and the rare-earth halide molecules considered in this work have relatively low ionization energies (about 6 eV). Therefore, the degree of ionization of the considered gases can become significant, depending on the gas density, even at temperatures below 10 000 K. This can be seen when studying ionization of the Dy atoms and DyBr molecules, which have the lowest (of all the particles considered here) ionization energies: 47 900 cm^{-1} and 46 900 cm^{-1}, respectively. Assuming that gas particle density N_0 is 2.7×10^{19} cm^{-3}, the degree of ionization x of the Dy gas in thermal (Saha) equilibrium is about 0.1 (at $T = 7000$ K) and 0.6 (at $T = 10\,000$ K). The corresponding values of x in the DyBr gas are 0.06 and 0.4, respectively. (One should remember that x is proportional to $N_0^{-1/2}$, whereas the electron density N_e is proportional to $N_0^{1/2}$. Thus, an increase of the gas density N_0 by an order of magnitude causes an increase of the electron density only by a factor of 3.) In general, a gas with a degree of ionization higher than about 0.1 should be considered a highly ionized gas, that is, a gas in which the presence of charged particles cannot be ignored. Such highly ionized gas (plasma) should be treated, during calculations of the gas thermodynamic functions, as a mixture of neutral and charged particles. Also, the high density of electrons in the gas causes the plasma properties to be dominated not by the binary collisions but by the collective interactions of the electric charges. Properties of such "coupled" plasma differ substantially from those described by the thermodynamic or kinetic models of the collision-dominated plasmas. The transition from the collisional plasma to the "coupled" plasma occurs when the potential energy U_D of the interaction between two plasma charges separated by a distance close to the Debye radius r_D becomes close to, or greater than, the mean thermal energy $3kT/2$ of the charges. The energy U_D can be given as

$$U_D \approx \frac{e^2}{r_D} = e^3 \left[\frac{4\pi N_e}{kT} \right]^{1/2} , \tag{46}$$

where e is the elementary charge and k is the Boltzmann constant.

As said before, a plasma containing singly charged particles will not be a "coupled" plasma if $U_D \ll kT$, that is, if

$$N_e \ll \frac{(kT)^3}{4\pi e^6} \quad \text{or} \quad N_e \ll 10^{19}(kT)^3 , \tag{47}$$

where N_e is given in cm^{-3} and kT in eV.

The importance of the Debye radius in the above discussion results from the fact that in most plasmas the number of charged particles in the Debye sphere centered around a charge is sufficient for an effective screening of the Coulomb interaction of the charge with another charge at a distance not smaller than the Debye radius. In such a case, the interaction between the two charges is through the Debye potential, which is of much shorter range than the Coulomb potential. Consequently, the interaction of the two charges at the distances $r \gtrsim r_D$ can be treated as a binary collision (if $U_D \ll kT$), and the equilibrium properties of the plasma can be obtained from thermodynamic or kinetic models of the ideal gas. If the density of plasma electrons is high, then, according to relationship (46), the potential energy U_D of the two charges can become comparable to, or greater than, the mean thermal energy of the charges. In such a case, the requirement (47) is not fulfilled—the plasma is "coupled" and it cannot be treated within the framework of the statistical mechanics of ideal gases.

The density of electrons in partially ionized and electrically neutral gas in Saha equilibrium is

$$N_e = 10^{11} N_0^{1/2} (kT)^{3/4} \exp(-V_{\text{ion}}/2kT)(2q_i/q_n)^{1/2} , \tag{48}$$

where N_e and N_0 are given in cm^{-3}, and kT and V_{ion} (the first ionization potential of the neutral particles) in eV, and where q_n and q_i are partition functions of the neutral particles and their singly charged ions, respectively. Combining requirement (47) and Eq. (48), one can say that partially ionized plasma is not "coupled" if the particle density in the plasma at temperature T is

$$N_0 \ll 10^{16}(kT)^{9/8} \exp(V_{\text{ion}}/kT)(q_n/2q_i) \ . \tag{49}$$

The value of the right-hand side of relationship (49) in the Dy gas is about 6×10^{19} cm^{-3} (at $T = 7000$ K) and 4×10^{18} cm^{-3} (at $T = 10\,000$ K). In the case of the DyBr gas, these values are 6.5×10^{18} cm^{-3} (at $T = 7000$ K) and 5×10^{17} cm^{-3} (at $T = 10\,000$ K). We assumed in our calculations that, in the Dy gas, $q_n/q_i \approx 1$, and in the DyBr gas, $q_n/q_i \approx 7$. [The corresponding values of the right-hand side of the relationship (49) are somewhat higher in the case of the other gases considered in this work.]

Summarizing the above discussion, one can say that the present approach is valid in the intended applications in the study of typical rare-earth light sources. In high-density, highly ionized rare-earth halide plasmas, the present approach may lead to inaccurate values of the partition functions. This results from the fact that such plasmas should be treated as nonideal plasmas (dominated by many-body interactions), in which the assumptions of the ideal-gas canonical and grand canonical distributions are unjustified. In addition, in highly ionized plasmas, the contribution of the scattering state to the total partition function becomes important [23]. Also, in dense plasma, some mechanisms other than those mentioned here should be included in calculations of thermodynamic properties of the plasma [24–26].

ACKNOWLEDGMENTS

This work was supported by the National Science Foundation through Grant No. CHE91-20339 for the Chemistry Department of the Massachusetts Institute of Technology, through a grant for the Institute for Theoretical Atomic and Molecular Physics at Harvard University and Smithsonian Astrophysical Observatory, and through ZRIF Grant No. 22-1514-9445. L.A.K. thanks the National Academies of Science of the USSR and of the United States for financial support.

---

*Present address: Department of Chemistry, Emory University, Atlanta, Georgia 30322.

†Present address: Department of Aerospace Engineering and Department of Physics, University of Southern California, Los Angeles, California 90089-1191.

[1] J. A. Kunc and W. H. Soon, Phys. Rev. A **40**, 5822 (1989).

[2] W. H. Soon and J. A. Kunc, Phys. Rev. A **43**, 723 (1991).

[3] D. R. Bates, Adv. At. Mol. Opt. Phys. **27**, 1 (1991).

[4] H. R. Griem, *Plasma Spectroscopy* (McGraw-Hill, New York, 1964).

[5] W. C. Martin, R. Zalubas, and L. Hagan, *Atomic Energy Levels: The Rare Earth Elements,* Natl. Bur. Stand. (U.S.) Circ. No. 60 (U.S. GPO, Washington, DC, 1978).

[6] R. W. Field, Ber. Bunsenges. Phys. Chem. **86**, 771 (1982).

[7] S. F. Rice, H. Martin, and R. W. Field, J. Chem. Phys. **82**, 1 (1985).

[8] L. A. Kaledin, J. G. Block, M. McCarthy, and R. W. Field, in *Proceedings of the 47th International Symposium on Molecular Spectroscopy,* edited by T. A. Miller (The Ohio State University, Columbus, 1992).

[9] L. A. Kaledin, C. Linton, B. Simard, T. E. Clarke, K. Beyea, and R. W. Field, in *Proceedings of the 47th International Symposium on Molecular Spectroscopy* (Ref. [8]).

[10] Z. B. Goldschmidt, in *Handbook of the Physics and Chemistry of Rare Earths,* edited by K. A. Gschneidner and L. Eyring (North-Holland, Amsterdam, 1978), p. 1.

[11] L. L. Ames, P. N. Walsh, and D. White, J. Phys. Chem. **71**, 2707 (1967).

[12] S. Smoes, P. Coppens, C. Bergman, and J. Drowart, Trans. Faraday Soc. **65**, 682 (1968).

[13] K. P. Huber and G. Herzberg, *Molecular Spectra and Molecular Structure IV: Constants of Diatomic Molecules* (Van Nostrand Reinhold, New York, 1979).

[14] E. Z. Zasorin, Russ. J. Phys. Chem. **62**, 883 (1988).

[15] L. A. Kaledin, E. J. Hill, and R. W. Field, in *Proceedings of the 46th International Symposium on Molecular Spectroscopy,* edited by N. K. Rao (The Ohio State University, Columbus, 1991).

[16] I. S. Gotkis, J. Phys. Chem. **95**, 6086 (1991).

[17] E. A. Shenyavskaya and L. V. Gurvich, J. Mol. Spectrosc. **81**, 152 (1980).

[18] L. V. Gurvich, I. V. Veyts, and C. B. Alcock, *Thermodynamic Properties of Individual Substances* (Hemisphere, New York, 1989).

[19] L. D. Landau and E. M. Lifshitz, *Statistical Physics* (Pergamon, Oxford, 1978).

[20] J. A. Kunc and W. H. Soon, Astrophys. J. **396**, 364 (1992).

[21] G. Ecker and W. Kroll, Phys. Fluids **6**, 62 (1963).

[22] J. A. Kunc, Phys. Rev. A **45**, 7851 (1992).

[23] F. J. Rogers, Astrophys. J. **310**, 723 (1986).

[24] G. B. Zimmerman and R. M. More, J. Quant. Spectrosc. Radiat. Transfer **23**, 517 (1980).

[25] W. Dappen, L. Anderson, and D. Mihalas, Astrophys. J. **319**, 195 (1987).

[26] D. G. Hummer and D. Mihalas, Astrophys. J. **331**, 794 (1988).

[27] L. Brewer, J. Opt. Soc. Am. **61**, 1666 (1971).

[28] R. M. Clements and R. F. Barrow, J. Mol. Spectrosc. **107**, 119 (1984).

[29] L. V. Gurvich, Yu. N. Dmitriev, L. A. Kaledin, A. I. Kobyliansky, A. N. Kulikov, and E. A. Shenyavskaya, Bull. Acad. Sci. USSR (Phys. Ser.) **53**, 75 (1989).

[30] D. J. Lumley and R. F. Barrow, J. Mol. Spectrosc. **69**, 494 (1978).

[31] L. A. Kaledin, C. Linton, T. E. Clark, and R. W. Field, J. Mol. Spectrosc. **154**, 417 (1992).